*Coordinatively unsaturated [RhCp*Rf$_2$] (Cp* = C$_5$Me$_5$; Rf = C$_6$F$_3$Cl$_2$-3,5), general precursor to Cp*-Diaryl and Cp*-Halo-Aryl Rh^{III} complexes. Observing and testing the effect of Cp* as electronic-buffer*

Marconi N. Peñas-Defrutos, Camino Bartolomé,* Pablo Espinet*

IU CINQUIMA/Química Inorgánica, Facultad de Ciencias, Universidad de Valladolid, 47071-Valladolid (Spain)

E-mail: espinet@qi.uva.es

http://gircatalisishomogenea.blogs.uva.es/

Supporting Information Placeholder

ABSTRACT: The pentacoordinated [RhCp*Rf$_2$] (Rf = C$_6$F$_3$Cl$_2$-3,5) and the octahedral (μ-Cl)$_2$[RhCp*Rf]$_2$, obtained by stoichiometric rearrangement with (μ-Cl)$_2$[RhCp*Cl]$_2$, are general precursors of [RhCp*RfXL] (X = Rf, Cl; L = ligand) complexes, which were studied by NMR (L dissociation and fluxional processes) and X-ray diffraction (structural effects affecting the Rh–Cp* distances) techniques. The Rh–Cp*centroid distance decreases markedly for identical L in the order [RhCp*Rf$_2$L] > [RhCp*RfClL] > [RhCp*Cl$_2$L], and are further influenced regularly within each family by the *trans influence* of L (longer distances for higher *trans influence* of L). The structural effects observed reveal a remarkable capability of Cp* to act as an electron-density buffer, which attenuates the Rh electron density variations induced by the substituents in front of Cp* by releasing towards Rh or polarizing towards Cp*, at demand, electron density of the Rh–Cp* bonds. This *buffer-effect* explains the easy L dissociation from [RhCp*Rf$_2$L] and the accessibility to formally 16e pentacoordinated [RhCp*Rf$_2$].

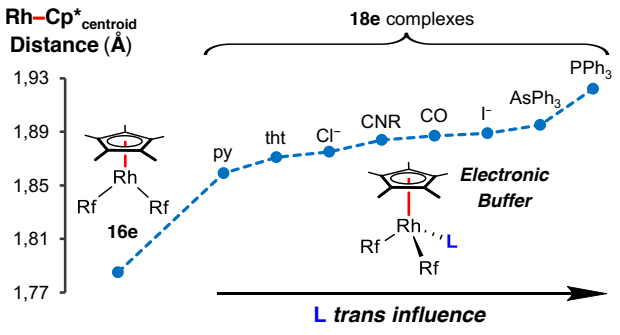

INTRODUCTION

Pentamethylcyclopentadienyl (Cp*) rhodium and iridium complexes, having as main precursor the dimer (μ-Cl)$_2$[MCp*Cl]$_2$ (M = Rh, Ir), were first made available by the group of Maitlis, by a reaction involving Dewar hexamethylbenzene ring contraction.[1,2] The synthesis was later improved to a procedure based on the deprotonation of pentamethylcyclopentadiene, which requires reflux for 21–48 h.[3] A modern modification using microwave techniques has reduced this time to 5-10 minutes.[4] More recently a similar procedure giving rapid access to ring substituted (μ-Cl)$_2$[MCp**Cl]$_2$ (Cp** = C$_5$Me$_4$R) complexes has been reported.[5] The MCp* moiety provides remarkable stability, solubility, easy NMR observation, and crystallinity to their complexes while the other three coordination positions are available to reactivity. Many recent catalytic studies confirm the present interest in MCp* complexes,[6] amongst them their use in C–H activation processes.[7]

RhCp* complexes are very predominantly octahedral 18e molecules, but a few have been reported that are pentacoordinated [RhCp*(L-L')] and contain a L-L' chelate ligand with the RhLL' metallacycle laying in a coordination plane perpendicular to the Cp* plane. The first paper on such species was the catecholate complex [RhCp*(O$_2$C$_6$H$_4$)], which exhibited deep blue color due to ligand-to-metal charge transfer (LMCT).[8] A number of related [RhCp*(E$_2$C$_6$H$_4$)] (E = O, S, NR) complexes have been reported since then (Figure 1, **A**).[9] These formally 16e complexes are in fact stabilized by π-donation from lone pairs on E, as identified by NBO analysis of some of the diamido complexes.[10] This means that it is more correct to say that they are not true 16e complexes, although they can function in some respects as if they were. For instance, pentacoordinated MCp* (M = Rh, Ir) complexes with chelate ligands combining amido-amino or amido-pyridyl groups (Figure 1, **B**) have been thoroughly studied in the group of Carmona, both structurally and in their interesting reactivity towards small molecules (CO, H$_2$, ethylene).[11,12,13,14] The reactions start by coordination of the small molecule (while the amido group retracts its lone electron pair) to give an octahedral intermediate.[15] A similar analysis had been applied earlier to explain the stability of a T-shaped tricoordinated [Pd^{II}(amido)XL], formally 14e but in fact closer to 16e complex.[16] In all these cases it can be useful to speak of *"functionally 14e"* tricoordinated Pd^{II} or *"functionally 16e"* pentacoordinated Rh^{III} complexes, respectively, because the complexes have ligands (e.g. the amido group) able to inject or recover electron density on demand.

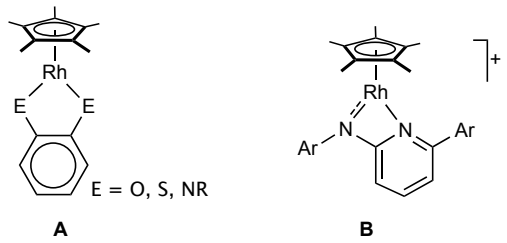

Figure 1. Pseudo-16e pentacoordinated RhCp* complexes.

Another remarkable class of transition metal organometallics is that of complexes with fluorinated haloaryls. Compared to common aryl ligands, haloaryls provide higher stability, slower reactivity, and easy ^{19}F NMR observation useful for mechanistic and structural studies. Interesting examples of multiarylation with haloaryls in rhodium(III) are the dianion $[Rh(C_6F_5)_5]^{2-}$ and the homoleptic complex $[Rh(C_6Cl_5)_3]$, which were prepared using lithium or, respectively, magnesium reagents.[17] The second complex is octahedral with κ^2(C,Cl)-chelating C_6Cl_5 groups. $[Rh(C_6F_5)_5]^{2-}$ has a square pyramidal structure. The reason for this stable pentacoordination was not discussed in the original paper, although probably the electronic richness of the dianionic Rh destabilizes the empty 4d and 5p orbitals of Rh enough as to make the metal center a very poor electrophile towards further coordination.

Compounds combining two organometallic functionalities, Cp* and R, are less common. Eighteen-electron [RhCp*RXL] (R = alkyl, aryl) complexes with piano-stool structures have been obtained by very different routes, such as: alkyl transfer from Mg,[6c,18] or B,[6c] derivatives; oxidative addition of C_6F_5I[19] or iodoperfluorocarbons[20] to Rh^I complexes; and thermal or photochemical activation of perfluorobenzene.[21] Some 18e [RhCp*R_2L] complexes have also been reported: [RhCp*Me_2(L)] (L = DMSO, PPh_3, dppm), using Al_2Me_6 as methylating agent,[22] and [RhCp*MeR(L)] (L = DMSO, CO), derived from them by reaction with arenes (releasing methane),[23] or aldehydes (releasing additionally DMSO and producing CO derivatives);[24] [RhCp*Me_2(py)], using $ZnMe_2$ as methylating agent;[25] [RhCp*(alkynyl)$_2$(PR_3)][6c,26] using alkynyl lithium; and [RhCp*($C_{12}H_8$)L] ($C_{12}H_8$ = *o*,*o*'-biphenylene; L = CO, dibenzotellurophene), using $Te(C_{12}H_8)$.[27]

Formally sixteen-electron pentacoordinated complexes with two carbyl ligands, [RhCp*R_2], are a rarity. A singular bis-*o*-carborane complex [RhCp*($C\{CB_{10}H_{10}\}_2$], defined as 16e pseudo-aromatic has been reported.[28] Pentacoordinated bisarylated RhCp*Ar_2 derivatives have not been reported until our recent communication of 16e [RhCp*Ar_2] (Ar = C_6F_5 = Pf ; Ar = $C_6F_3Cl_2$-3,5 = Rf).[29] Finally, one amido-type C,N-cyclometallated complex [RhCp*(C–N)],[6a] and a cationic $[RhCp^*(C–S)]^+$ where a 2,6-dimesitylbenzenethiolate ligand displays mesityl C1 π-coordination to Rh,[30] have also been published.

Coming back to our 16e [RhCp*Ar_2] complexes, they were obtained using as arylating agent the corresponding $[AgAr]_n \cdot n$NCMe compound and (μ-Cl)$_2$[RhCp*Cl]$_2$ (**1**), taking advantage of the insolubility of silver halides (Scheme 1).[29,31] The deep garnet 16e complex [RhCp*Rf_2] (**2**) was directly obtained from the reaction, while the corresponding 18e yellow [RhCp*Pf_2(NCMe)] (**3**) was obtained in the same reaction conditions (Scheme 1) because the Rh center is slightly more acidic with Pf as aryl and retains the acetonitrile coming with the silver reagent. Deep garnet 16e [RhCp*Pf_2] can be obtained from **3** by controlled heating to eliminate the coordinated. MeCN.

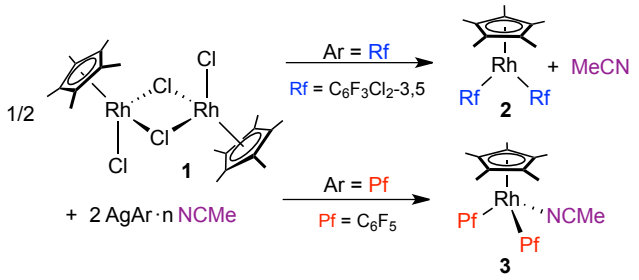

Scheme 1. Synthesis of 16e and 18e RhCp*Ar_2 complexes. corrected

The study of solutions containing a 1:1 mixture of [RhCp*Rf_2] (**2**) and [RhCp*Pf_2] uncovered an aryl exchange process, which was not direct but catalyzed by an unobservable amount of [RhCp*Ar(OH)]. The later comes from dissociation of *syn*-(μ-OH)$_2$[RhCp*Ar]$_2$, which is formed in solution by slow hydrolysis of [RhCp*Ar_2].[29] This study left open some questions about the stability and behavior as Lewis acid of these 16e [RhCp*Ar_2] complexes, and their possible use as Ar transmetalating reagents.[32] These questions are dealt with here. For the present study, Ar = Rf has been preferred because it shows a slightly higher tendency to pentacoordination, and because of the simplicity of its ^{19}F spectra.

RESULTS AND DISCUSSION

The Lewis acidity of [RhCp*Rf_2]. Synthesis of diaryl RhCp* octahedral complexes. The reactivity of **2** with neutral or anionic ligands is shown in Scheme 2. Overall the reactions suggest a latent weak and soft acidic behavior towards sixth coordination (for instance, THF does not coordinate but tetrahydrothiophene does). Although the formal oxidation state of the metal center is Rh^{III}, the Cp* group is strongly electron donor and the aryl groups are also strong σ donors compared to halides,[33] which makes the Rh^{III} center in **2** relatively electron rich. In fact, it refuses to coordinate weak donor ligands with hard donor atoms such as THF or OH_2 that, however, coordinate to other Rh^{III} cationic systems with higher electrophilicity.[34,7c] In contrast, **2** accepts stronger and softer neutral ligands to give the corresponding isolable complexes **4**-**10**.

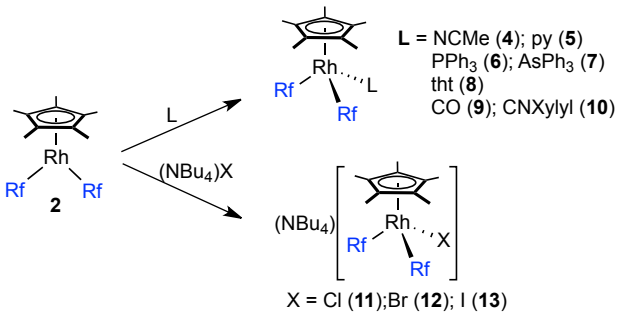

Scheme 2. Reactivity of [RhCp*Rf_2] (2) towards anionic and neutral ligands: Synthesis of bisarylated complexes 4-13.

The molecular structure of [RhCp*Rf_2(PPh_3)] (**6**), depicted in Figure 2, shows that the two aryl rings are non-equivalent. Those of [RhCp*Rf_2(py)] (**5**), [RhCp*Rf_2($AsPh_3$)] (**7**) and [RhCp*Rf_2(tht)] (**8**) are shown in Figures S2, S5, and S6, respectively.

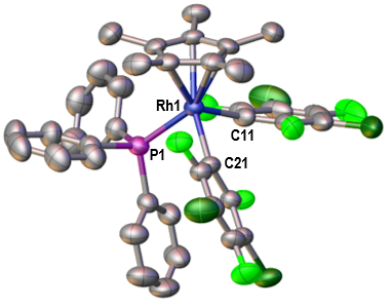

Figure 2. X-Ray structure of [RhCp*Rf_2(PPh_3)] (**6**). H atoms omitted for clarity. Selected bond lengths (Å): Rh(1)–C(11) = 2.105(4); Rh(1)–C(21) = 2.136(4); Rh(1)–P(1) = 2.3482(12). Selected bond angles (°): C(11)–Rh(1)–C(21) = 89.91(19); C(11)–Rh(1)–P(1) = 101.96(16); C(21)–Rh(1)–P(1) = 86.64(13).

The reactions of **2** with CO or CNXylyl give [RhCp*Rf_2(CO)] (**9**) or [RhCp*Rf_2(CNXylyl)] (**10**), respectively. Both complexes are remarkably stable and do not show any sign of ligand dissociation in solution. The isocyanide complex is also resistant to migratory insertion and to nucleophilic attack by $NHMe_2$. In the IR spectra complex **9** shows an intense band at ν_{CO} = 2064 cm^{-1} (ν_{CO} = 2143 cm^{-1} in free CO), and complex **10** one at ν_{CN} = 2151 cm^{-1} (ν_{CN} = 2120 cm^{-1} in free CNXylyl). The meaning of these values is commented later.

The X-ray diffraction structures of [RhCp*Rf_2(CO)] (**9**) (Figure 3, left) and [RhCp*Rf_2(CNXylyl)] (**10**) (Figure 3, right) confirm the expected coordination of the ligands.

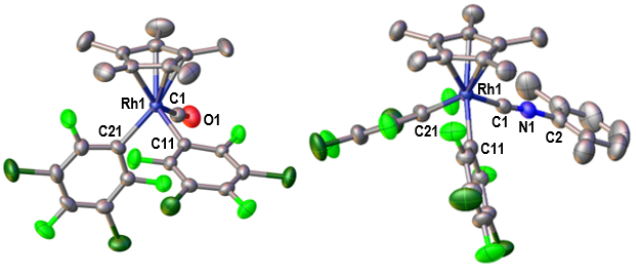

Figure 3. Left: X-Ray structure of [RhCp*Rf_2(CO)] (**9**). H atoms omitted for clarity. Selected bond lengths (Å): Rh(1)–C(11) = 2.072(5); Rh(1)–C(21) = 2.110(5); Rh(1)–C(1) = 1.879(5); C (1)–O(1) = 1.137(6). Selected bond angles (°): C(11)–Rh(1)–C(21) = 86.4(2); C(11)–Rh(1)–C(1) = 97.0(2); C(21)–Rh(1)–C(1) = 87.8(2); Rh(1)–C(1)–O(1) = 172.4(5). Right: X-Ray structure of [RhCp*Rf_2(CNXylyl)] (**10**). H atoms omitted for clarity. Selected bond lengths (Å): Rh(1)–C(11) = 2.112(3); Rh(1)–C(21) = 2.058(3); Rh(1)–C(1) = 1.935(3); C(1)–N(1) = 1.157(3); N(1)–C(2) = 1.406(4). Selected bond angles (°): C(11)–Rh(1)–C(21) = 85.84(10); C(11)–Rh(1)–C(1) = 88.97(11); C(21)–Rh(1)–C(1) = 95.63(11); Rh(1)–C(1)–N(1) = 171.7(3); C(1)–N(1)–C(2) = 172.3(3).

The reaction of [RhCp*Rf_2] (**2**) with (NBu_4)X salts (X = I, Br, Cl) in acetone (Scheme 2) produces (NBu_4)[RhCp*Rf_2X] (**11-13**). The molecular structure of the iodide derivative **13** is shown in Figure 4. In contrast with the numerous examples of cationic RhCp* complexes, complexes **11-13** are among the rare examples of anionic RhCp* complexes reported. The anionic character of the ligands does not work in favor of their coordination to a fairly electron rich center. In fact, stirring crystals of (NBu_4)[RhCp*Rf_2I] (**13**) or the other halide complexes in methanol or ethanol washes away (NBu_4)I to regenerate **2**, confirming the high stability of the 16e precursor and the poor coordination of the halides.

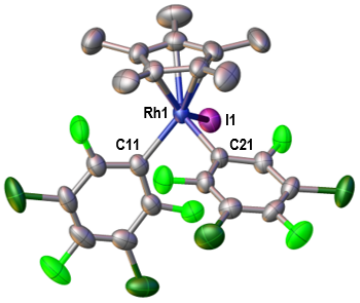

Figure 4. X-Ray structure of (NBu_4)[RhCp*Rf_2I] (**13**). H atoms omitted for clarity. Selected bond lengths (Å): Rh(1)–C(11) = 2.112(3); Rh(1)–C(21) = 2.067(4); Rh(1)–I(1) = 2.7585(4). Selected bond angles (°): C(11)–Rh(1)–C(21) = 85.36(14); C(11)–Rh(1)–I(1) = 89.59(10); C(21)–Rh(1)–I(1) = 101.80(10). H atoms omitted for clarity.

The coordination of the entering ligands is instantaneous in all the reactions performed (Scheme 2), always accompanied by the same dramatic color change from the deep garnet of [RhCp*Rf_2] (**2**) to orange or yellow, depending on the ligand used (Figure S13). A strong LMCT band at 505 nm (molar extinction coefficient = 780 $M^{-1}cm^{-1}$) is responsible for the color of **2** but it is absent in the 18e complexes. UV-vis data in CH_2Cl_2 for **2** and **9** are given in the SI.

All the complexes **4-8** and **11-13**, show dichroic behavior in solution due to dissociation equilibria (Eq 1). Their ^{19}F NMR spectra show that, at low temperature (below 250 K) these equilibria are highly displaced to the left (only the non-dissociated [RhCp*Rf_2L] is observed). This large equilibrium shift with temperature supports that the ΔH_{eq} contribution to ΔG_{eq} is unexpectedly small in general, and the equilibrium displacement is largely under entropy control. This provokes that, for instance, the solutions in CH_2Cl_2 of [RhCp*Rf_2(NCMe)] (**4**) are deep garnet (color corresponding to large dissociation to **2**) at room temperature, but become yellow (color of complex **4**) at low temperature (200 K). The *apparently* thermochromic behavior of **4** is in reality the effect of temperature on the concentration of the 5- and 6-coordinate species in solution.[35]

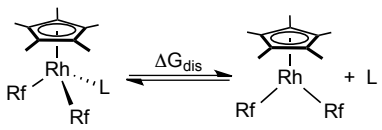

(1)

For the PPh_3 (**6**) or $AsPh_3$ (**7**) complexes the spectroscopic studies by ^1H, ^{19}F, and (when available) ^{31}P NMR show that the exchange rates of equilibrium are slow at room temperature in the NMR timescale. The three components of the equilibrium can be individually observed at room temperature and integrated. The slowness of the process preserves the coupling

constants through the Rh–L bonds that are broken. [36] In addition, broadening of some bands reveal fluxional phenomena associated to restricted rotation, which were studied at variable temperature.[18] As the most informative case, the behavior of the PPh_3 complex **6** is discussed. The case of **7** is very similar.

Figure 5 shows the ^{19}F NMR spectra of a solution of **6** in CD_2Cl_2 at different temperatures At 305 K (blue spectrum) the F_o and F_p signals of **6** and the coordinatively unsaturated **2** can be distinguished separately, with integration of the corresponding peaks affording **2**:**6** ≈ 1:3 ratio. This is confirmed in the ^{31}P spectrum where free and coordinated PPh_3 are observed in the same 1:3 ratio and the coordinated PPh_3 signal is a doublet ($^1J_{P\text{-}Rh}$ = 142.8 Hz). However, only one broad F_o and one sharp F_p signals are observed, indicating that the two non-equivalent Rf groups seen in the X-ray structure of **6** (Figure 2) are being interconverted (still too slowly for the F_o signal). At 200K (red spectrum) the signals of **2** are not observed, and only coordinated PPh_3 is shown in the ^{31}P spectrum, confirming total equilibrium displacement towards [RhCp*Rf_2(PPh_3)] (**6**). Interestingly, the fluxional processes affecting the molecule at 305 K have been frozen efficiently at 200K, and the ^{19}F NMR spectrum has collapsed to the pattern predicted for a structure with two non-equivalent Rf groups: two F_p signals, and four F_o signals, revealing that the non-equivalent Rf groups can only tilt around the Rf–Rh bond but full rotation is hindered. Consequently the two non-equivalent F_o atoms on each Rf group are give rise to four signals. Restricted rotation around the Rh–PPh_3 is confirmed in the aromatic region of ^1H NMR spectra at 200 K (Figure S3). Other restricted rotations about M–PR_3 bonds in stereochemically crowded systems have been reported,[37] and activation barriers to M–C*ipso* rotation in different fluoroaryl complexes have been studied.[18,38] The only movement that remains fully active at 200 K is Cp*–Rh rotation, which produces five equivalent Me groups, in contrast with the solid-state condition. The large difference between the chemical shifts of the F_o signals for the two components (about 10 ppm) is noticeable, and it is always observed for all the coordinatively saturated [RhCp*Rf_2L] complexes synthesized.

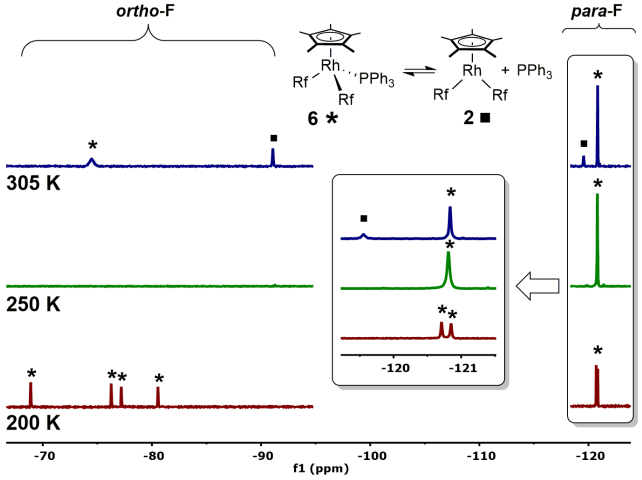

Figure 5. ^{19}F NMR spectra of [RhCp*Rf_2(PPh_3)] (**6**) in CD_2Cl_2 at different temperatures. An expansion of the F_p region is shown in the frame.

At 250 K (Figure 5, green line) the ^{19}F NMR spectrum shows that ligand dissociation has already become very thermodynamically disfavored, to the point that only **6** is observed. The two F_p singlets, very close in chemical shift, are already above their coalescence temperature showing a slightly broadened signal. The F_o signals are not observed because they are in the range of their coalescence temperature. At 305 K these signals have already coalesced to a broad singlet.

The dissociation equilibrium for the py complex **5** is much faster (Figure S1). This complex, as well as **9** and **10**, having ligands with less steric requirement, show free rotation of the Rf group at least down to 200K. Some spectroscopic studies are provided in the SI.

Synthesis of monoarylated derivatives (μ-Cl)$_2$[RhCp*Rf]$_2$ (14) and [RhCp*RfClL] (15-19). Whereas different procedures for the synthesis of aryl halo complexes [RhCp*RXL] have been reported, none of them affords a general precursor.[19,21] Having observed fast aryl exchange between [RhCp*Ar_2] complexes, catalyzed by *syn*-(μ-OH)$_2$[RhCp*Rf]$_2$ we hypotezised that complex [RhCp*Rf_2] (**2**) should be a good arylating candidate to transfer an aryl group to Rh^{III} haloderivatives. Indeed, the reaction of **1** with (μ-Cl)$_2$[RhCp*Cl]$_2$ yields quantitatively (μ-Cl)$_2$[RhCp*Rf]$_2$ (**14**) (Scheme 3). In view of the transition state for Ar/OH transmetalation calculated in our previous study,[29] *anti*-(μ-Cl)(μ-Rf)[RhCp*Rf][RhCp*Cl] can be proposed as transmetalation transition state for Rf/Cl rearrangement.

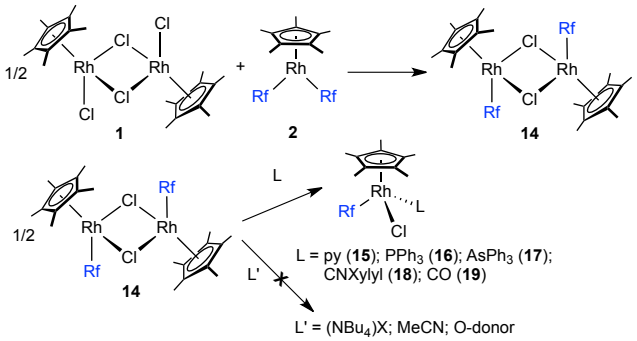

Scheme 3. Symmetrization between [RhCp*Rf_2] and (μ-Cl)$_2$[RhCp*Cl]$_2$ to obtain monoarylated compounds.

The molecular structure of complex **14** is shown in Figure 6.[39] The asymmetric unit is only one-half of the dimer. The Rf aryls are mutually *anti* in the crystal studied. This is the only isomer observed by ^1H and ^{19}F NMR in solutions made at 213 K in $CDCl_3$, confirming that the whole solid is *anti*. Upon warming, a *syn*:*anti* = 1:7 equilibrium is formed, and the unequivocal assignment of the signals of both isomers could be made (Figure 7). In CD_2Cl_2 the equilibrium ratio is different (*syn*:*anti* =1:2.4) due to the change of solvent polarity.

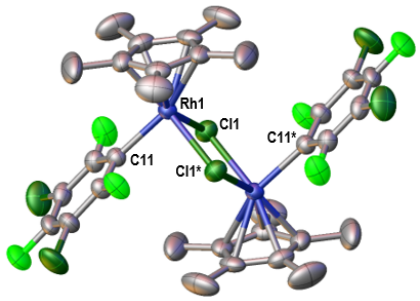

Figure 6. X-Ray structure of *anti*-(μ-Cl)$_2$[RhCp*Rf]$_2$ (**14**). H atoms omitted for clarity. Selected bond lengths (Å): Rh(1)–C(11)

= 2.072(3); Rh(1)–Cl(1) = 2.4328(8); Rh(1)–Cl(1*) = 2.4497(8). Selected bond angles (°): C(11)–Rh(1)–Cl(1) = 90.46(8); C(11)–Rh(1)–Cl(1*) = 90.97(8); Cl(1)–Rh(1)–Cl(1*) = 83.08(3).

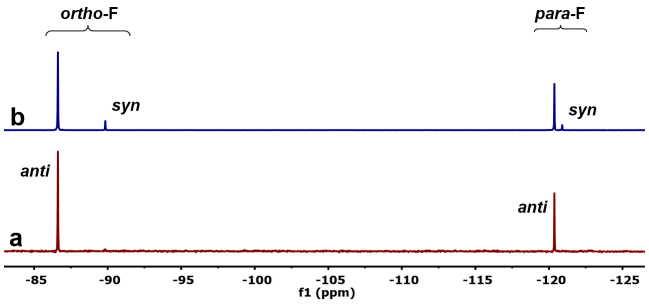

Figure 7. a) ^{19}F NMR spectrum of a sample of **14** dissolved in $CDCl_3$ at 213 K. **b)** The same sample left to reach room temperature and then cooled down to 213 K.

Bridge splitting with different ligands (L = CO, CNXylyl, py, PPh_3, $AsPh_3$) leads to [RhCp*RfClL] complexes (**15-19**). These were characterized by NMR spectroscopy and by single crystal X-Ray diffraction studies (Figures S9-S13).

Interestingly, attempts at producing [RhCp*RfClL] failed for L = MeCN or X^-. Although these ligands formed [RhCp*Rf_2L] complexes and the Rh center in **14** might be expected to be more acidic (the substitution of one Rf for one more electronegative Cl increases the acidity of the sixth coordination position), the splitting of the Cl bridges in the dimer is thermodynamically unfavorable for these weak ligands. In contrast the reaction works for stronger σ-donor ligands, including isocyanide, yielding complexes **16-18**. The case is less clear for L = CO when weak σ-donation needs to be synergistically reinforced with strong back-donation. The fact is that coordination of CO in **19** is easily reversed under vacuum, regenerating **14**, in contrast to the high stability of **9** in the same conditions.

The suspect that the Rh center should be less electron rich and more acidic in [RhCp*RfClL] than in [RhCp*Rf_2L] complexes might be examined looking at the ν(CN) or ν(CO) stretching frequencies in the corresponding complexes. For the isocyanide complexes the ν_{CN} wavenumbers follow the trend [RhCp*Cl_2(CNXylyl)][40] (2172 cm^{-1}) > [RhCp*RfCl(CNXylyl)] (2159 cm^{-1}) > [RhCp*Rf_2(CNXylyl)] (2151 cm^{-1}), which confirm that the higher ν_{CN} appear when coordinated to the expectedly less electron rich Rh center. This is also the case for the trend in carbonyl complexes ([RhCp*Cl_2(CO)] does not exist): [RhCp*RfCl(CO)] (2067 cm^{-1}) > [RhCp*Rf_2(CO)] (2064 cm^{-1}). Yet the very small variation in wavenumbers is a bit surprising and its meaning will be considered later in the paper.

The NMR behavior of the [RhCp*Rf_2L] complexes and their [RhCp*RfClL] analogs confirms many similarities but also reveals some unexpected differences. For instance, the restriction to Rf rotation observed in the biaryl complex with PPh_3 (**6**) upon cooling also operates in the mono-aryl complex **16**, as observed in Figure 8, in this case at room temperature. At variance with **6**, where only were $J_{Me\text{-}P}$ = 2.8 Hz and $^1J_{Rh\text{-}P}$ = 142.8 Hz are detected, in complex **16** $J_{Me\text{-}P}$ = 3.2 Hz and $^1J_{Rh\text{-}P}$ = 144.2 Hz, but also $^3J_{Fo\text{-}Rh}$ = 6.0 Hz and $^4J_{Fo\text{-}P}$ = 19.3 Hz coupling to one of the two non-equivalent F_o,[41] are observed. This coupling system gives rise to the doublet of doublets in Figure 8. The observation of the two additional couplings in **16** is somehow in line with the expectations of stronger Rh–L bonds compared to **6**, even if the increase of coupling constant values is minimal. Perhaps the more striking evidence is that PPh_3 dissociation equilibrium in CD_2Cl_2 is measurable for **6** and undetectable for **16**. Assuming that a signal of 2% intensity might be detected by NMR this roughly this suggests that the stability of **16** vs. **14** is at least about 3 kcal mol^{-1} higher than the stability of **6** vs. **2**. Due to the very different structures of **2** and **14** this estimated ΔG_{dis} difference cannot be attributed to the different strengths of the corresponding Rh–PPh_3 bonds.

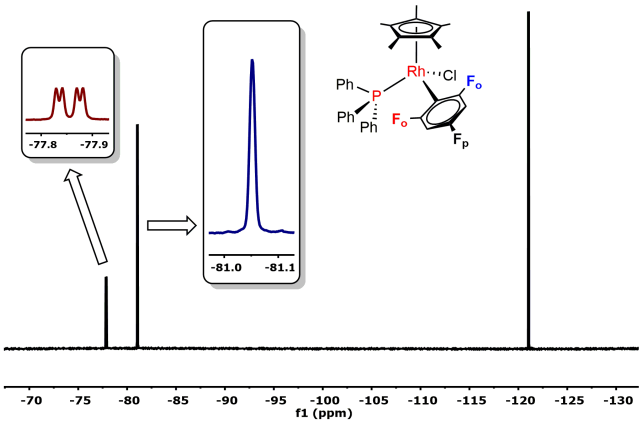

Figure 8. ^{19}F NMR spectra of [RhCp*RfCl(PPh_3)] (**16**) at 293 K.

The spectra of complex [RhCp*RfCl(CNXylyl)] (**18**) are interesting because Rf rotation is frozen in the NMR timescale at 200K (Figure 9). In the analogous complex **10** this rotation could not be frozen in the same conditions, which strongly supports that the chloro ligand imposes higher steric hindrance to rotation than a second Rf group. Similar to Figure 8, the spectra in Figure 9 show two non-equivalent F_o nuclei below coalescence, with only one of them presenting $^4J_{Rh\text{-}F}$ (8.4 Hz). Above coalescence the signals become equivalent and the $^4J_{Rh\text{-}F}$ coupling averages to 4.4 Hz.

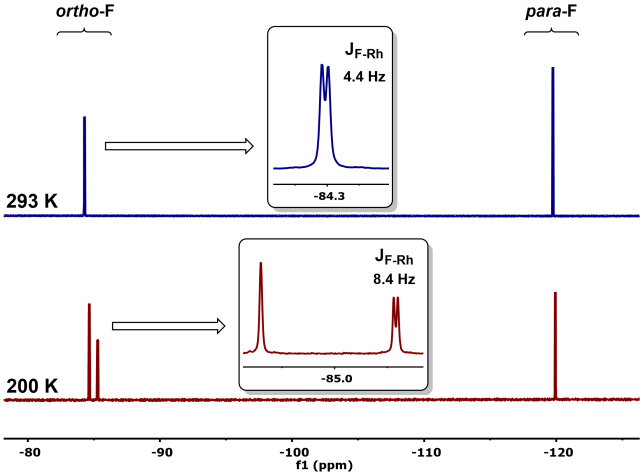

Figure 9. ^{19}F NMR spectra of **18** at 293 K and 200 K.

The comments above, about the expected strengthening of the Rh–L bonds upon replacement of one Rf for one Cl group, might find a reflect in the corresponding bond distances. The data in Table 1, from X-ray studies in this work or in the refer-

ences mentioned, reveal interesting variations as the number of electronegative Cl (chloro) groups increases.[42] For L = py, the Rh–L distance progressively decreases, as expected. For PPh_3 and $AsPh_3$, the effect is almost negligible. For the strong π acceptor CO and CNXylyl ligands, the bond length increases. This can be understood as an effect of increasing electrophilicity of the metal center when more electronegative Cl (cloro) groups replace good σ-donor Rf groups. The progressive replacement is favorable for σ-donating ligands (entry 5), detrimental for large π-back-acceptor ligands (entry 1 < entry 2), and almost neutral for ligands with both components more balanced (entries 3 and 4).

Entry	L	$RhCp^*Rf_2L$	RhCp*RfClL	$RhCp^*Cl_2L$
1	CO	1.879(5)	1.907(7)	–
2	CNXylyl	1.935(3)	1.949(5)	1.9675(14)[40]
3	PPh_3	2.3482(12)	2.3505(6)	2.3439(5)[6d]
4	$AsPh_3$	2.4580(11)	2.4555(3)	2.4440(13)[43]
5	py	2.155(3)	2.152(4)	2.127(2)[44]

Table 1. Rh–L bond distances (Å) in $[RhCp^*Rf_2L]$, [RhCp*RfClL], and $[RhCp^*Cl_2L]$ complexes.

Remarkable role of Cp* as electron-density buffer. The availability of a high number of structures from the previous sections allows us to make some structural observations that can be analyzed qualitatively assuming that the structural features observed are the consequence of each molecule having achieved its optimal electron-density distribution.[45] Basically, it is the electron density in orbitals in the valence shell that is involved. We propose as a simple approximation that a 18e transition metal center, contributing to the system many electrons and a nucleus with many protons, is very much defining its own electronic density contour, which will not be prone to be much altered upon coordination or dissociation of one ligand, if ligands facilitating delocalization and polarization are accessible to keep this density contour more constant.[46] This is exactly the basis of the structural *trans influence* phenomenon (strong σ donors elongate the bonds in trans position to their coordination positions), studied mostly in square-planar Pt^{II} complexes.[47] In fact this *trans influence* was explained by a polarization theory as early as 1935.[48] Applied to octahedral complexes $[RhCp^*X_2L]$ (X_2 = Rf_2, RfCl, Cl_2) the Rh center will tend to minimize externally induced electron density changes, by polarizing electron density through their bonds to these ligands. Note that in this qualitative approach we are not specifying orbitals, and we are considering the electron density as a whole being susceptible of delocalization and polarization.

With these simple premises in mind we can check, to start with, how the 5-coordinate complexes **2** (an atypical example of **A** in Figure 1), and **20** (a typical example of **B** in Figure 1) respond to the incorporation of an entering ligand (Scheme 4). Complex **2** is an example 5-coordination stabilized by two strongly σ-donor Rf ligands; it is likely that the fluorinated aryl will be only scarcely able to provide some π donation to Rh, and this is why we call it atypical compared to the so far available 5-coordinate complexes **A**. Complex **20**, however, produces important π donation from the amido N atom to Rh, which is reflected in an appreciable shortening of the N–Rh bond. Both complexes, **2** and **20**, have their octahedral partners with the ligands Cl^- (chloride) or CNXylyl. The N–Rh distance in **20** (1.98 Å) elongates to 2.11 Å (a single N–Rh bond distance) in **21**-**22** upon ligand coordination.[13,14] In contrast, L coordination to **2** scarcely affects the Rf–Rh bond distances in **10**-**11**: the most different Rf–Rh distances, 2.06 and 2.11 Å, are found in the octahedral complex **10**, while the distances in the pentacoordinated **2** are 2.06 and 2.07 Å. All these Rh–C distances are consistent with single bonds as reported for fluoroaryl-Rh^{III} complexes.[17,49]

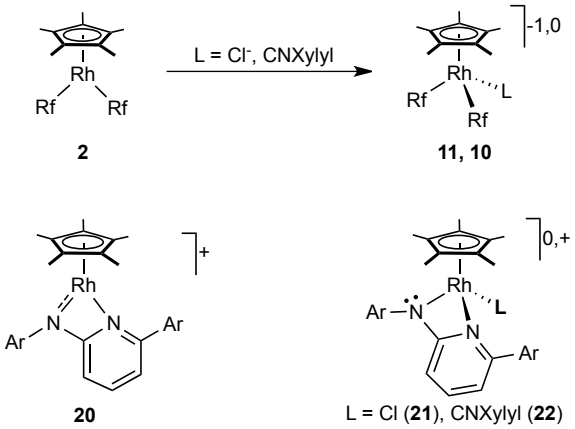

Scheme 4. Coordination of Cl^- or CNXylyl to two kinds of pentacoordinated RhCp* complexes.

Table 2 collects the Rh–Cp*centroid distances (distances to the geometrical center of the Cp*) for the six complexes in Scheme 4 and highlight how much they change upon coordination of Cl^- or CNXylyl (**Δd**). Comparing entries 2 and 5, corresponding to Cl^- coordination, we see that **Δd** is close to zero in **21** but quite large (0.090 Å) in **11**. We could say that, as the Cl^- nucleophile approaches Rh, complex **21** fully compensates the additional electron density brought to Rh by the entering Cl^- by giving back to N the π electron density that had been delocalized into Rh to stabilize complex **20**. This electron density returns to the most stable N orbital and the overall electronic effect on Rh is almost neutral. For the better donor CNXylyl in **22**, this compensation is not enough and the Rh atom polarizes some additional electron density towards Cp*, which elongates the Rh–Cp*centroid distance, as shown in Table 2. For complexes **11** and **10** the coordination of L produces in both cases much larger elongations of the Rh–Cp*centroid distance, suggesting that the Rf group is simply a strong σ-donor that cannot respond to L coordination,[50] and all the electron-density compensation around Rh has to be made by delocalizing and polarizing more electron density of the Rh–Cp* bonds (which involve soft π and π* aromatic Cp* orbitals) towards Cp*.

Entry	Compd.	$d_{Rh\text{-}Cp^*centroid}$ (Å)	**Δd** (Å)	Reference
1	**20**	1.769(4)	-	13
2	**21**	1.772(4)	+0.003	13
3	**22**	1.802(3)	+0.033	13
4	**2**	1.785(4)	-	this work
5	**11**	1.875(3)	+0.090	this work
6	**10**	1.884(3)	+0.099	this work

Table 2. The effect of L coordination on Rh-Cp*centroid distance.

Since Cp* undergoes free rotation in solution (interconverting their five C atoms), and also in order to simplify the comparison of data, we decided to use Rh–Cp*centroid distances for the analysis of the X-ray characterized RhCp* complexes, as applied above and later. However, the whole set of X-ray structures available shows that the five C atoms of Cp* can be far from being equidistant from Rh. Moreover, they show distances that can be related to the structural effect associated to the well-known *trans influence* of ligands, observed in square planar complexes. For instance, in complex [RhCp*Rf_2(tht)] (**8**) the X-ray structure shows two slightly different molecules. The data for one of them (the other is similar) has a Cp* carbon atom almost exactly trans to the S atom of tht, with $d_{Rh–C}$ = 2.191(4) Å. Each position trans to the Rf carbons is almost the center of the bond of a pair of Cp* carbon atoms, with distances d_{Rh-C} = 2.256(4), 2.253(4) Å for one pair, and d_{Rh-C} = 2.232(5), 2.222(4) Å for the other. The largest distances are found trans to the Rf groups, which have higher trans influence than tht.

We examine now the wide collection of Rh–Cp*centroid data gathered in Figure 10, including data for [RhCp*Rf_2L], [RhCp*RfClL], and [RhCp*Cl_2L] complexes. Note that all the complexes are octahedral but their precursors differ: Complex **2** is pentacoordinated and L coordination only requires a structural rearrangement, but complexes **1** and **14** are octahedral with Cl-bridges and L coordination requires splitting these bridges, which is somehow equivalent to a ligand substitution reaction. Upon L coordination to the octahedral complexes **1** and **14** the Rh atom will lose electron density from the bridging Cl (which was acting as the 2e ligand making the split bond) and will gain electron density from the new incoming 2e L ligand, hence it looks reasonable that in these two series the Rh center should gain less electron density upon L coordination than in the octahedral complexes derived from the pentacoordinated **2**. In order to keep relatively unaltered the electronic density around Rh, a structural change occurs in the three cases, affecting the Rh–Cp*centroid distance. As expected, the elongation of the Rh–Cp*centroid distance in the complexes derived from **2**, which have gained more incoming electron density upon L coordination, is larger than in those originated by bridge-for-L substitutive-splitting. In fact, this is clearly observed comparing the initial step of the three lines in Figure 10.

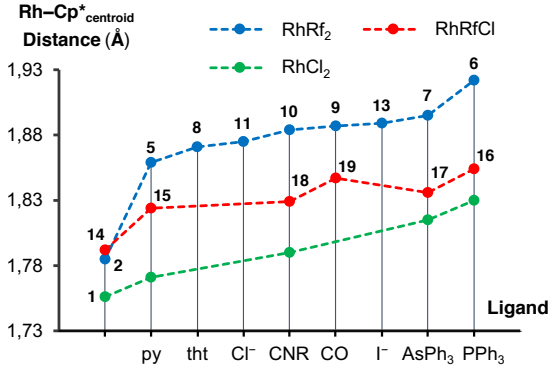

Figure 10. Plot of Rh–Cp*centroid distances in complexes reported in this paper (blue and red lines) or in the literature (green line).[6d,40,43,44]

On the other hand, we could expect that the ligands donating more overall electron density to Rh should produce also longer Rh–Cp*centroid distances, more or less following the order of *trans influence* series available in the literature.[47,48] In fact this is the case in the three series.[51] Moreover, after the first step the three series run reasonably parallel. Overall, it seems that the relationship between Rh–Cp*centroid distance and ligand *trans-influence* makes much sense. Finally, the relative positions of the three series clearly reflect the expected decrease in overall electron density donated by the R or X groups and the L ligand (overall electron density $RhRf_2L$ > RhRfClL > $RhCl_2L$), which is compensated on Rh by producing shorter Rh–Cp*centroid distances as Rf groups are replaced by more electronegative Cl (chloro) groups. Other examples in the literature fit this analysis. For instance, the Rh–Cp*centroid distance is larger in [RhCp*PhCl(PPh_3)][6d] than in [RhCp*RfCl(PPh_3)] (**16**) (1.887(4) Å *vs.* 1.854(2) Å); or in [RhCp*Me_2(κS-DMSO)][25a] than in [RhCp*Rf_2(κS-tht)] (**8**) (1.890(4) Å *vs.* 1.871(4) Å).

All the data discussed so far are not in contradiction with the initial proposal that the Rh^{III} center in RhCp* complexes is comfortable with an electron density environment that will be kept fairly constant as much as their ligands allow for structural changes that minimize the effect of the disturbing forces. In this respect, the π-bonded ligands provide a higher flexibility because they can rearrange electron density in the molecule with less energetic cost. As we have seen, the π electron density of the N_{amido}–Rh bond is the first resource used by Carmona's complex **20** to accommodate the entering ligand and keep the electronic density in the proximity of the Rh center with just little variation. When this is not possible (as in our complexes), or when it is not sufficient, the abundant and soft π electron density of Cp* is easily delocalized and polarized towards the Cp* domain to produce a similar effect. Thanks to this high polarizability, Cp* is able to behave as a powerful electron-density buffer, simply by changing the bond distances to Rh. The practical consequence of this is that the loss of electron density around the metal center upon dissociation of one ligand from the 18e octahedral complex can be attenuated by shortening the Rh–Cp*centroid distance. In other words, the hipothetical 18e/16e switch in the electron count around Rh does not represent the real variation and dissociative processes (the usual way octahedral processes start their reactions) are facilitated in RhCp* complexes compared to RhCp homologues because Cp* is better donor than Cp.

This electronic-buffer effect can be compared to the well known *"indenyl effect"*, thoroughly examined in the last two decades of the 20th century.[52] It was proposed to explain how 18e indenyl complexes undergo associative ligand substitution reactions much faster than their cyclopentadienyl homologues. The main reason is that the indenyl complexes can facilitate the attack of nucleophiles without increasing the electron count on the metal center, by means of an easy slippage of the metal from η^5- to η^3-bonded; this slippage is energetically compensated in part by the increase of aromaticity in the six-membered ring and avoids a much higher in energy 20e transition state. The cyclopentadienyl (Cp) complexes probably follow a similar pattern but, lacking this possibility of aromaticity compensation, have much higher activation energy val-

ues for associative processes. However, Cp* is richer in electron density and softer than Cp and, according to our analysis, the Cp* complexes do have an efficient way to mitigate large changes of electron density in the valence shell of Rh by shifting the Cp* ring closer or farther away from Rh, as required (Scheme 5).

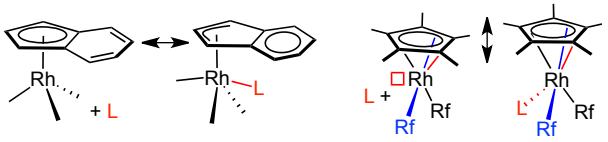

Scheme 5. "18e to 18e" structural conversions facilitating ligand association (Left: indenyl effect, Rh slippage) or dissociation (Right: Cp* buffering compensation).

CONCLUSIONS

The *functionally 16e* [RhCp*Rf_2] complex is an excellent starting material to obtain clean and selectively many bisarylated compounds. The comproportionation reaction between [RhCp*Rf_2] and (μ-Cl)$_2$[RhCp*Cl]$_2$ leads to the dimer (μ-Cl)$_2$[RhCp*Rf]$_2$, which is precursor of monoarylated [RhCp*RfClL] complexes. The study of many X-ray molecular structures offers data to observe structural effects in octahedral [RhCp*Rf_2L] and [RhCp*RfClL] complexes.

The analysis of the structures available suggests that the overall electron density changes, induced by the ligands (Rf, Cl, L) additional to Cp*, are counterbalanced by variations of Rh–Cp* bond distances that delocalize and polarize the electron density of the Rh–Cp*bonds, from or towards the Cp* group. This is the expected structural effect of the *trans influence* of the ligands, which translates the electronic polarization of a L–M bond to the M–L' bond in trans position. This structural effect is also produced upon exchange of Rf (more donor) for Cl (chloro, more electronegative) groups, which shortens the Rh–Cp* distance as the number of more electronegative Cl groups increases. Thus, an interesting feature of the *buffer effect* of Cp* is that it provides infrequent experimental observations of the structural *trans influence* of ligands in octahedral complexes.

The reactivity of 18e octahedral complexes, usually starting by L dissociation, is facilitated by the high buffer effect of Cp*. This is clearly supported by the fact that L dissociation from [RhCp*Rf_2L] is very efficient for ligands that, in other circumstances, should require very different dissociation energies. Furthermore, a most interesting extrapolation for reactivity is that the buffer effect of Cp* should be able to influence reactions occurring at the other side of the molecule. It is reasonable to suggest that, in reactions taking place in the three reactive positions in front of Cp*, the energy differences between intermediates and transition states may be somehow shortened by influence of the *buffer effect*, and reactions occurring on RhCp* complexes might benefit from lower activation energies than, for instance, reactions occurring on RhCp moieties.

ASSOCIATED CONTENT

Supporting Information

PDF (36 pages): Synthesis and full characterization of the complexes, additional data and X-ray structures.
The Supporting Information is available free of charge on the ACS Publications website.

The crystallographic data for this paper, CCDC 1833306-1833319, are freely available from the Cambridge Crystallographic Data Centre.

AUTHOR INFORMATION

Corresponding Authors

* Pablo Espinet phone (+34)983186336; e-mail, espinet@qi.uva.es; web, http://cinquima.uva.es
* Camino Bartolomé (experimental): phone (+34)983184521; e-mail, caminob@qi.uva.es;

ORCID

Pablo Espinet: 0000-0001-8649-239X
Camino Bartolomé: 0000-0002-8492-6825
Marconi N. Peñas-Defrutos: 0000-0003-4804-8751

Author Contributions

All the authors have contributed to the manuscript and have given approval to the final version.

Notes

The authors declare no competing financial interest.

ACKNOWLEDGMENTS

Thanks are given to the Spanish MINECO projects CTQ2016-80913-P, CTQ2014-52796-P, and CTQ2017-89217-P; the Junta de Castilla y León (VA051P17); and the Spanish MECD for a FPU grant (M. N. Peñas-Defrutos).

DEDICATION

We are very happy to congratulate Ernesto Carmona, an outstanding example of the best Inorganic and Organometallic Spanish Chemistry, on occasion of his birthday. He may be officially 70 from now on, but he is *functionally 40* in research.

REFERENCES

[1] (a) Kang, J. W.; Mosley, K.; Maitlis, P. M. The mechanisms of the reactions of Dewar hexamethylbenzene with rhodium and iridium chlorides. *Chem. Commun.* **1968**, *21*, 1304–1305. (b) Kang, Jung W.; Maitlis, P. M. Conversion of Dewar hexamethylbenzene to pentamethylcyclopentadienylrhodium(III) chloride. *J. Am. Chem. Soc.* **1968**, *90*, 3259–3261. (c) Kang, J. W.; Moseley, K.; Maitlis, P. M. Pentamethylcyclopentadienylrhodium and -iridium halides. I. Synthesis and properties. *J. Am. Chem. Soc.* **1969**, *91*, 5970–5977.

[2] Maitlis, P. M. Pentamethylcyclopentadienyl)rhodium and -iridium complexes: approaches to new types of homogeneous catalysts. *Acc. Chem. Res.* **1978**, *11*, 301–307.

[3] (a) White, C.; Yates, A.; Maitlis, P. M.; Heinekey, D. M. (η^5-Pentamethylcyclopentadienyl)Rhodium and Iridium Compounds. *Inorg. Synth.* **1992**, *29*, 228–234. (b) Du, Y.; Hyster, T. K.; Rovis, T. Rhodium(III)-catalyzed oxidative carbonylation of benzamides with carbon monoxide. *Chem. Commun.* **2011**, *47*, 12074–12076. (c) Fujita, K.; Takahashi, Y.; Owaki, M. Yamamoto, K.; Yamaguchi, R. Synthesis of Five-, Six-, and Seven-Membered Ring Lactams by Cp*Rh Complex-Catalyzed Oxidative N-Heterocyclization of Amino Alcohols. *Org. Lett.* **2004**, *6*, 2785–2788.

[4] Tönnemann, J.; Risse, J.; Grote, Z.; Scopelliti, R.; Severin, K. Efficient and Rapid Synthesis of Chlorido-Bridged Half-Sandwich Complexes of Ruthenium, Rhodium, and Iridium by Microwave Heating. *Eur. J. Inorg. Chem.* **2013**, 4558–4562.

[5] Brown, L. C.; Ressegue, E.; Merola, J. S. Rapid Access to Derivatized, Dimeric, Ring-Substituted Dichloro(cyclopentadienyl) Rhodium(III) and Iridium(III) Complexes. *Organometallics* **2016**, *35*, 4014–4022.

[6] (a) Wu, Q.; Chen, Y.; Yan, M.; Lu, Y.; Sun, W.-Y.; Zhao J. Unified synthesis of mono/bis-arylated phenols *via* Rh^{III}-catalyzed dehydrogenative coupling. *Chem. Sci.* **2017**, *8*, 169–173. (b) Yu, X.; Duan, Y.; Guo, W.; Wang, T.; Xie, Q.; Wu, S.; Jiang, C.; Fan, Z.; Wang, J.; Liu, G. Rhodium-Catalyzed Oxidative Decarboxylation Annulation Reactions of Mandelic Acids and Alkynes: An Efficient Synthetic Method for Indenones. *Organometallics* **2017**, *36*, 1027–1034. (c) Martínez de Salinas, S.; Díez, J.; Falvello, L. R.; González, J.; Gamasa M. P.; Lastra, E. Intramolecular C–C Coupling Reactions of Alkynyl, Vinylidene, and Alkenylphosphane Ligands in Rhodium(III) Complexes. *Organometallics* **2016**, *35*, 2793–2805. (d) Lau, Y.-F.; Chan, C.-M.; Zhou, Z.; Yu, W.-Y. Cp*Rh(III)-catalyzed electrophilic amination of arylboronic acids with azo compounds for synthesis of arylhydrazides. *Org. Biomol. Chem.* **2016**, *14*, 6821–6825. (e) Xie, F.; Qi, Z.; Yu, S.; Li, X. Rh(III)- and Ir(III)-Catalyzed C–H Alkynylation of Arenes under Chelation Assistance *J. Am. Chem. Soc.* **2014**, *136*, 4780–4787. (f) Zhang, H.; Wang, K.; Wang, B.; Yi, H.; Hu, F.; Li, C.; Zhang, Y.; Wang J. Rhodium(III)-Catalyzed Transannulation of Cyclopropenes with *N*-Phenoxyacetamides through C–H Activation *Angew. Chem. Int. Ed.* **2014**, *53*, 13234–13238. (g) Shi, Y.; Blum, S. A. *Organometallics* **2011**, *30*, 1776–1779.

[7] For C–H activation, see: (a) C Kuhl, N.; Schröder, N.; Glorius, F. Formal S_N-Type Reactions in Rhodium(III)-Catalyzed C–H Bond Activation. *Adv. Synth. Catal.* **2014**, *356*, 1443–1460. (b) Colby, D. A.; Tsai, A. S.; Bergman, R. G.; Ellman, J. A. Rhodium Catalyzed Chelation-Assisted C–H Bond Functionalization Reactions. *Acc. Chem. Res.* **2012**, *45*, 814–825. See also some selected reports: (c) Zhang, G.; Yang, L.; Wang, Y.; Xie, Y.; Huang, H. An Efficient Rh/O_2 Catalytic System for Oxidative C–H Activation/Annulation: Evidence for Rh(I) to Rh(III) Oxidation by Molecular Oxygen. *J. Am. Chem. Soc.* **2013**, *135*, 8850−8853. (d) Martínez, A. M.; Echavarren, J.; Alonso, I.; Rodríguez, N.; Gómez Arrayás, R.; Carretero, J. C. Rh^{I}/Rh^{III} catalyst-controlled divergent aryl/heteroaryl C–H bond functionalization of picolinamides with alkynes. *Chem. Sci.* **2015**, *6*, 5802–5814. (e) Thenarukandiyil, R.; Thrikkykkal, H.; Choudhury, J. Rhodium(III)-Catalyzed Nonaromatic sp^2 C–H Activation/Annulation Using NHC as a Directing and Functionalizable Group. *Organometallics* **2016**, *35*, 3007–3013.

[8] Espinet, P.; Bailey, P. M.; Maitlis, P. M. Pentamethylcyclopentadienyl-rhodium and iridium complexes. Part 22. Blue five-co-ordinate rhodium(III) complexes derived from catechol and related compounds. *J. Chem. Soc., Dalton Trans*. **1979**, 1542–1547.

[9] (a) Holland, A. W.; Glueck, D. S.; Bergman, R. G. Photochemical Reactivity of Group 9 Metal Pinacolate Complexes. *Organometallics* **2001**, *20*, 2250–2261. (b) Paek, C.-K.; Ko, J.-J.; Uhm, J.-K. Synthesis and Characterization of 1,4-Diimine Complexes of 1,2,3,4,5-Pentamethylcyclopentadienylrhodium and iridium. *Bull. Korean Chem. Soc.* **1994**, *15*, 980–984. (c) Shibata, Y.; Zhu, B.; Kume, S.; Nishihara, H. Development of a versatile synthesis method for trinuclear Co(III), Rh(III), and Ir(III) dithiolene complexes, and their crystal structures and multi-step redox properties. *Dalton Trans.* **2009**, 1939–1943. (d) Liu, J.-J.; Lin, Y.-J.; Jin, G.-X. A stepwise assembly of a molecular box from 16-electron half-sandwich precursors [Cp*M(pdt)] (M = Rh, Ir). *Dalton Trans*. **2015**, *44*, 10281–10288. (e) Han, Y.-F-; Zhang, L.; Weng, L.-H.; Jin, G.-X. H_2−Initiated Reversible Switching between Two-Dimensional Metallacycles and Three-Dimensional Cylinders. *J. Am. Chem. Soc.* **2014**, *136*, 14608−14615.

[10] Blacker, A. J.; Clot, E.; Duckett, S. B.; Eisenstein, O.; Grace, J.; Nova, A.; Perutz, R. N.; Taylor, D. J.; Whitwood, A. C. Synthesis and structure of ''16-electron'' rhodium(III) catalysts for transfer hydrogenation of a cyclic imine: mechanistic implications. *Chem. Commun.* **2009**, 6801–6803.

[11] Zamorano, A.; Rendón, N.; López-Serrano, J.; Valpuesta, J. E. V.; Álvarez, E.; Carmona, E. Dihydrogen Catalysis of the Reversible Formation and Cleavage of C–H and N–H Bonds of Aminopyridinate Ligands Bound to $(\eta^5\text{-}C_5Me_5)Ir^{III}$. *Chem.–Eur. J.* **2015**, *21*, 2576–2587.

[12] Valpuesta, J. E. V.; Rendón, N.; López-Serrano, J.; Poveda, M. L.; Sánchez, L.; Álvarez, E.; Carmona, E. Dihydrogen-Catalyzed Reversible Carbon–Hydrogen and Nitrogen–Hydrogen Bond Formation in Organometallic Iridium Complexes. *Angew. Chem. Int. Ed.* **2012**, *51*, 7555–7557.

[13] Zamorano, A.; Rendón, N.; Valpuesta, J. E. V.; Álvarez, E.; Carmona, E. Synthesis and Reactivity toward H_2 of $(\eta^5\text{-}C_5Me_5)Rh(III)$ Complexes with Bulky Aminopyridinate Ligands. *Inorg. Chem.* **2015**, *54*, 6573–6581.

[14] Zamorano, A.; Rendón, N.; López-Serrano, J.; Álvarez, E.; Carmona, E. Activation of Small Molecules by the Metal–Amido Bond of Rhodium(III) and Iridium(III) $(\eta^5\text{-}C_5Me_5)M$-Aminopyridinate Complexes. *Inorg. Chem.* **2018**, *57*, 150–162.

[15] For the shake of brevity other structures with two chelating heteroatoms structurally that can be related to **A** or **B** are not mentioned, , but a recent Rh example with infrequent N,O chelating coordination, and the interesting reactivity of Ir phosphoramidate complexes can be mentioned: Drover, M. W.; Love, J. A.; Schafer, L. L. Toward anti-Markovnikov 1-Alkyne O-Phosphoramidation: Exploiting Metal−Ligand Cooperativity in a 1,3-N,O-Chelated Cp*Ir(III) Complex. *J. Am. Chem. Soc.* **2016**, *138*, 8396−8399.

[16] (a) Moncho, S.; Ujaque, G.; Lledós, A.; Espinet P. When Are Tricoordinated Pd^{II} Species Accessible? Stability Trends and Mechanistic Consequences *Chem.–Eur. J.* **2008**, *14*, 8986–8994. (b) Moncho, S.; Ujaque, G.; Espinet, P.; Maseras, F.; Lledós, A. The role of amide ligands in the stabilization of Pd(II) tricoordinated complexes: is the Pd-NR_2 bond order single or higher?. *Theor. Chem. Acc.* **2009**, *123*, 75–84.

[17] (a) García, M. P.; Oro, L. A.; Lahoz, F. J. Novel Anionic Aryl Complexes of Rh^{III}: $[Rh(C_6F_5)_5]_2^-$ and $[Rh(C_6F_5)_4(CO)_2]^-$. *Angew. Chem. Int. Ed. Engl.* **1988**, *27*, 1700–1702. (b) García, M. P.; Jiménez, M. V.; Lahoz, F. J.; López, J. A.; Oro, L. A. Synthesis of the homoleptic rhodium(III) complex $[Rh(C_6Cl_5)_3]$. Molecular structures of $[Rh(C_6Cl_5)_3]$ and $[Rh(C_6Cl_4\text{–}C_6Cl_4)(C_6Cl_5)(SC_4H_8)_2]$. *J. Chem. Soc. Dalton Trans.* **1998**, 4211–4214.

[18] Jones, W. D.; Feher, F. J. Preparation and conformational dynamics of $(C_5Me_5)Rh(PR^1{}_3)RX$. Hindered rotation about rhodium-phosphorus and rhodium-carbon bonds. *Inorg. Chem.* **1984**, *23*, 2376–2388.

[19] Hughes, R. P.; Laritchev, R. B.; Williamson, A.; Incarvito, C. D.; Zakharov, L. N.; Rheingold, A. L. Iridium and Rhodium Complexes Containing Fluorinated Phenyl Ligands and Their Transformation to η^2-Benzyne Complexes, Including the Parent Benzyne Complex $IrCp^*(PMe_3)(C_6H_4)$. *Organometallics* **2002**, *21*, 4873−4885.

[20] Gil-Rubio, J.; Guerrero-Leal, J.; Blaya, M.; Vicente, J.; Bautista, D.; Jones, P. G. Reactions of Half-Sandwich Ethene Complexes of Rhodium(I) toward Iodoperfluorocarbons: Perfluoro-alkylation or -arylation of Coordinated Ethene versus Oxidative Addition. *Organometallics* **2012**, *31*, 1287–1299.

[21] (a) Edelbach, B. L.; Jones, W. D. Mechanism of Carbon−Fluorine Bond Activation by $(C_5Me_5)Rh(PMe_3)H_2$. *J. Am. Chem. Soc.* **1997**, *119*, 7734−7742. (b) Belt, S. T.; Helliwell, M.; Jones, W. D.; Partridge, M. G.; Perutz, R. N. η^2-Coordination and carbon-fluorine activation of hexafluorobenzene by cyclopentadienylrhodium and -iridium complexes. *J. Am. Chem. Soc.* **1993**, *115*, 1429−1440. (c) Jones, W. D.; Partridge, M. G.; Perutz, R. N. Sequential arene coordination and C–F insertion in the reactions of $(\eta^5$-pentamethylcyclopentadienyl)rhodium complexes with hexafluorobenzene. *J. Chem. Soc., Chem. Commun.* **1991**, 264–266.

[22] Vázquez de Miguel, A.; Gómez, M.; Isobe, K.; Taylor, B. F.; Mann, B. E.; Maitilis, P. M. Reactions of Dichlorobis(μ-chloro)

bis(pentamethylcyclopentadienyl)dirhodium and -diiridium with Hexamethyldialuminum. *Organometallics* **1983**, *2*, 1724–1730.

[23] (a) Gómez, M.; Robinson, D. J.; Maitlis, P.M. Iridium(V) and rhodium (V) intermediates in aromatic metallation; the unusual reactivity of iodobenzene. *J. Chem. Soc., Chem. Commun*. **1983**, 825–826. (b) Gomez, M.; Yarrow, P. I. W.; Robinson, D. J.; Maitlis, P.M. A new aromatic metallation reaction involving rhodium and iridium; the unusual reactivity of iodobenzene. *J. Organomet. Chem.* **1985**, *279*, 115–130.

[24] Gómez, M.; Kisenyi, J. M.; Sunley, G. J.; Maitlis, P. M. Reaction of the rhodium and iridium complexes $[C_5Me_5MMe_2(Me_2SO)]$ with aldehydes to give $[C_5Me_5MMe(R)(CO)]$. *J. Organomet. Chem.* **1985**, *296*, 197–207.

[25] (a) Fooladi, E.; Graham, T.; Turner, M. L.; Dalhus, B.; Maitlis, P. M.; Tilset, M. Oxidatively induced M–C bond cleavage reactions of $Cp^*Ir(Me_2SO)Me_2$ and $Cp^*Rh(Me_2SO)Me_2$ ($Cp^* = \eta^5$-C_5Me_5). *J. Chem. Soc., Dalton Trans.* **2002**, 975–982. (b) Cadenbach, T.; Gemel, C.; Schmid, R.; Fischer, R. A. Mechanistic Insights into an Unprecedented C−C Bond Activation on a Rh/Ga Bimetallic Complex: A Combined Experimental/Computational Approach. *J. Am. Chem. Soc.* **2005**, *127,* 17068–17078.

[26] Ara, I.; Berenguer, J. R.; Eguizábal, E.; Forniés, J.; Lalinde, E.; Martín, A.; Martínez, F. Structural characterization of the acetylide bridge in dinuclear (μ-C≡CSiMe$_3$)-Al/Al and -Al/Zr complexes. *Organometallics*, **1998**, *17*, 4578–4596.

[27] Badyal, K.; McWhinnie, W. R.; Chen, H. L.; Hamor T. A. Heterocyclic organotellurium compounds as precursors for new organometallic derivatives of rhodium *J. Chem. Soc., Dalton Trans.* **1997**, 1579–1586.

[28] Yao, Z-J.; Zhang, Y-Y.; Jin, G-X. Pseudo-aromatic bis-o-carborane iridium and rhodium complexes. *J. Organomet. Chem.* **2015**, *798*, 274–277.

[29] Peñas-Defrutos, M. N.; Bartolomé, C.; García-Melchor, M.; Espinet, P. Hidden aryl-exchange processes in stable 16e Rh^{III} $[RhCp^*Ar_2]$ complexes, and their unexpected transmetalation mechanism. *Chem. Commun.* **2018**, *54*, 984–987.

[30] Sakamoto, M.; Ohki, Y.; Tatsumi, K. Synthesis and Reactions of Coordinatively Unsaturated Half-Sandwich Rhodium and Iridium Complexes Having a 2,6-Dimesitylbenzenethiolate Ligand. *Organometallics* **2010**, *29*, 1761–1770.

[31] The silver complexes $[Ag(C_6F_5)]_n$ and $[Ag(C_6F_5)_2]^-$ have been used before to obtain pentafluorophenyl complexes of several metal centers, including Rh^{III} and Rh^{I}: (a) García, M. P.; Jiménez, M. V.; Lahoz, F. J.; Oro, L. A. Synthesis and Reactivity of Mononuclear Anionic Pentafluorophenyl Compounds of Rhodium(I) and Iridium(I). X-ray Structure of $[\{P(OPh)_3\}_2(C_6F_5)_2RhAg(PPh_3)]$ *Inorg. Chem.* **1995**, *34*, 2153–2159. (b) Bennett, R. L.; Bruce, M. I.; Gardner, R. C. F. Polyfluoroaromatic derivatives of metal carbonyls. Part IX. Reactions of pentafluorophenylsilver(I) with some transition-metal halogeno-complexes; oxidative-addition reactions of the complex carbonyl(pentafluorophenyl)bis(triphenylphosphine)iridium(I). *J. Chem. Soc., Dalton Trans.* **1973**, 2653–2657.

[32] The C donor atom in these aryls has not lone pairs but only the aromatic π electron density of the Pf or Rf ring to stabilize pentacoordination versus octahedral coordination, if the strongly electron-withdrawing F substituents permit.

[33] For instance, although the electronegativity of C_6F_5 has been compared to that of Br, $C_6F_5^-$ shows a large *trans influence* in many X-ray structures of Pd complexes, while Br^- has a low *trans influence*.

[34] (a) Hughes, R. P.; Lindner, D. C.; Smith, J. M.; Zhang, D.; Incarvito, C. D.; Lam, K.-C.; Liable-Sands, L. M.; Sommer, R. D.; Rheingold, A. L. Water, water, everywhere. Synthesis and structures of perfluoroalkyl rhodium and iridium(III) compounds containing water ligands. *Dalton Trans.* **2001**, 2270−2278. (b) Brasse, M.; Cámpora, J.; Ellman, J. A.; Bergman, R. G. Mechanistic Study of the Oxidative Coupling of Styrene with 2-Phenylpyridine Derivatives Catalyzed by Cationic Rhodium(III) via C–H Activation. *J. Am. Chem. Soc.* **2013**, *135*, 6427–6430.

[35] The concept *thermochromism* is usually applied to color changes provoked by temperature changes due to phenomena conserving basically unaltered the molecular structure, which is not the case.

[36] Ligand dissociation was reported for the related 16e complex $[RhCp^*(O_2C_6H_4)]$ ($O_2C_6H_4$ = catecholate) and its 18e L complexes $[RhCp^*(O_2C_6H_4)L]$.[8] In that case, however, the coupling constants through the P–Rh bond were lost at room temperature (at 60 MHz) for L = PPh_3, but retained for L = PEt_3.

[37] Bartolomé, C.; Espinet, P.; Villafañe, F.; Giesa, S.; Martín, A.; Orpen, A. G. (2,4,6-Tris(trifluoromethyl)phenyl)palladium(II) Complexes. *Organometallics* **1996**, *15*, 2019–2028, and references therein.

[38] Espinet, P.; Albéniz, A. C.; Casares, J. A.; Martínez-Ilarduya, J. M. ^{19}F NMR in organometallic chemistry Applications of fluorinated aryls. *Coord. Chem. Rev.* **2008**, *252*, 2180–2208.

[39] A similar complex $(\mu\text{-Cl})_2[RhCpPf]_2$ was reported long ago, obtained by a totally different and less efficient synthetic route: Stone, F. G. A.; Mukhedkar, A. J.; Mukhedkar, V. A.; Green, M. Reactions of low-valent metal complexes with fluorocarbons. Part XIII. (π-Cyclopentadienyl)bis(π-ethylene)rhodium. *J. Chem. Soc. A* **1970**, 3158–3161.

[40] Walsh, A. P.; Brennessel, W. W.; Jones, W. D. Synthesis and characterization of a series of rhodium, iridium, and ruthenium isocyanide complexes. *Inorganica Chim. Acta* **2013**, *407*, 131–138.

[41] A similar observation was reported for $[RhCp^*(C_6F_5)X(PMe_3)]$ (X = Cl, I): (a) References 19 and 21c.

[42] The Cl (chloro) groups, which count for the Rh^{III} the oxidation state, should not be mistaken with the Cl^- (chloride) anionic ligand. The former contributes only 1e to the bond electron pair shared with Rh and, being Cl more electronegative, formation of this bond diminishes the electron density on Rh. The later contributes the 2e to bond formation, and one negative charge to the complex, increasing the electron density on Rh as any other donating ligand.

[43] Chalmers, B. A.; Bühl, M.; Nejman, P. S.; Slawin, A. M. Z.; Woollins, J. D.; Kilian, P. Rhodium(III) and iridium(III) half-sandwich complexes with tertiary arsine and stibine ligands. *J. Organomet. Chem.* **2015**, *799-800*, 70–74.

[44] Therrien, B.; Burrell, A. K. Di-chloro(η^5-pentamethyl-cyclo-pentadienyl)(pyridine-N)-rhodium. *Acta Cryst.* **2001**, *E57*, m259–m260.

[45] The optimal electron density distribution is the one that accomplishes better the Maximum Chemical Hardness Principle. See, for instance: (a) Pearson, R. G. The Principle of Maximum Hardness. *Acc. Chem. Res.* **1993**, *26*, 250–255. (b) Parr, R. G.; Zhou, Z. Absolute Hardness: Unifying Concept for Identifying Shells and Subshells in Nuclei, Atoms, Molecules, and Metallic Clusters. *Acc. Chem. Res.* **1993**, *26*, 256–258.

[46] For definition of electron delocalization and electron polarization in the context of density functional theory (DFT), Chemical Hardness, and the HSAB Principle see: R. G. Pearson. Chemical Hardness. Applications From Molecules to Solids. Wiley-VCH Veinheim, Germany (1997).

[47] Hartley F. R. The cis- and trans-Effects of Ligands. *Chem. Soc. Rev.* **1973**, *2*, 163–179.

[48] For modern comments on that theoretical proposal, hardly accessible in the original, see: J. E. Huheey. Inorganic Chemistry. Principles of Structure and Reactivity, SI units edition. Pages 423–429. Harper&Row, Publishers. London (1975).

[49] García, M. P.; Jiménez, M. V.; Lahoz, F. J.; Oro, L. A.; Tiripicchio, A.; López, J. A. Tris(pentafluorophenyl) neutral and anionic five-coordinate complexes of rhodium(III). Crystal structures of $[Rh(C_6F_5)_3(PEt_3)_2]$ and $[Rh(C_6F_5)_3(AsPh_3)_2]$. *J. Chem. Soc., Dalton Trans.* **1990**, 1503–1508.

[50] Hypothetically some aromatic electron density from the $C_6F_3Cl_2$-3,5 ring might be used to increase the Rh–Rf bond order in complex **2** and then be recovered in **11** and **10**, but the electronegative substituents make unlikely this contribution to be significant. Moreover, the large

Rh–Cp*centroid elongation observed confirms that it absorbs all the effect of ligand coordination.

[51] The location of the CO ligand is problematic due to strong σ,π synergistic effects upon coordination to different centers but, in the references given above, its position in the series is in coincidence with its position in Figure 10.

[52] Calhorda, M. J.; Romão, C. C.; Veiros, L. F. The Nature of the Indenyl Effect. *Chem.–Eur. J.* **2002**, *8*, 868–875.